EROSION OF UNPROTECTED CAUSEWAYS DUE TO WAVES

by

Nobuhisa Kobayashi

and

Robert A. Dalrymple

Sponsored by

University of Delaware

Sea Grant College Program

Research Report No. CE-86-58

September, 1986

OCEAN ENGINEERING PROGRAM

DEPARTMENT OF CIVIL ENGINEERING
UNIVERSITY OF DELAWARE
NEWARK, DELAWARE 19716

SUMMARY

Erosion of an unprotected gravel causeway due to breaking waves is analyzed. Using a new technique, analytical and numerical solutions are obtained for predicting erosion at the bend and tip of the causeway. Computation is made for a causeway in the southern Beaufort Sea.

EROSION OF UNPROTECTED CAUSEWAYS DUE TO WAVES

KEY WORDS: Erosion, Causeways, Waves, Coastal Engineering, Beaches, Sands

ABSTRACT:

An analysis is performed for erosion of an unprotected gravel causeway with a relatively gentle side slope caused by the variation of sediment transport rates along the causeway due to breaking waves. Use is made of the coordinate following the curved shoreline of the causeway and the longshore sediment transport formula developed for natural beaches. Neglecting wave refraction and diffraction, simple analytical and numerical solutions are obtained for predicting erosion at the bend and tip of the causeway. These solutions are used to compute erosion of a hypothetical causeway in the southern Beaufort Sea. The computation indicates that erosion due to an occasional severe storm may be severe but limited in the vicinity of the bend and tip of the causeway. The analysis also suggests that if a slope protection system is provided to a limited region of a causeway, erosion of the unprotected region next to the protected region could be similar to that of the tip of an unprotected causeway. However, field data is needed to verify and calibrate the proposed model based on the analogy between a gravel causeway and a natural sand spit.

TABLE OF CONTENTS

INTRODUCTION

Causeways have been used and proposed as pipeline shore-crossing corridors in the southern Beaufort Sea north of Alaska (2). Causeways will be subjected to wave and current action during the open water period of approximately three months each year. Large longshore sediment transport and beach volume changes during severe summer storms have been observed and predicted by a number of investigators (4,6,11,12,16). An unprotected causeway may hence suffer severe erosion but the cost of a protection system for a very long causeway may be prohibitive. A method for predicting the severity of erosion of an unprotected causeway is needed so as to determine an advantageous configuration of the causeway under site-specific storm conditions and evaluate the amount and frequency of maintenance requirements.

This paper presents an analysis for erosion of an unprotected causeway with relatively gentle side slopes caused by the variation of sediment transport rates along the causeway due to breaking waves. The mathematical formulation of the problem is similar to those used for the prediction of shoreline evolution (8,9,10,13,14) except that the present analysis utilizes the coordinate which follows a curved shoreline. A simple analytical solution is obtained for predicting the severity of erosion at the bend of a long causeway. Analytical and numerical solutions are also presented for predicting erosion and recession of the tip of a long causeway of finite width. These solutions neglect wave refraction and diffraction but are very easy to apply for a preliminary design of a causeway. Computation is made for a hypothetical causeway in the southern Beaufort Sea. The computed results are discussed in the light of the limitations of the present simple analysis.

FORMULATION OF THE PROBLEM

A causeway in the southern Beaufort Sea is normally constructed of gravel and may have a reasonably gentle side slope (e.g., 1:5). As a first approximation, the causeway may be regarded to be similar to a natural spit of finite width so that use may be made of the analysis procedures for predicting shoreline evolution (8,9,10,13,14). In the following, the shoreline of the causeway is defined as the intersecting line between the mean water level and the side slope of the causeway.

The shoreline location changes with time due to erosion or accretion caused by sediment transport along and perpendicular to the causeway. Fig. 1 shows the location of the curved shoreline exposed to wave attack at time t as well as some of the notation used in the paper. s is the coordinate following the curved shoreline whose positive direction is chosen such that the causeway is located on the left hand side of the coordinate s. (x,y) is the fixed Cartesian coordinate system. $\vec{m} = (\cos\beta, \sin\beta)$ is the unit tangential vector in the positive s-direction and $\vec{n} = (-\sin\beta, \cos\beta)$ is the unit normal vector into the causeway. β is the angle between $\vec{m}$ and the x-axis which is measured counterclockwise from the positive x-direction. α_b is the angle of wave incidence at the breaker point relative to the y-direction as shown in Fig. 1. Q is the volumetric longshore sediment transport rate and q_n is the volumetric offshore sediment transport rate per unit shoreline length. Using the notation of complex variables, the location of an arbitrary point on the curved shoreline at time t is expressed as

$$z_s = x_s + i\, y_s \tag{1}$$

in which i = the imaginary unit such that $i^2 = -1$, and (x_s, y_s) = the location of the point in terms of the Cartesian coordinate system. The location z_s varies

with time and with the coordinate s. The unit tangential and normal vectors at a given time are related to the variation of z_s along the coordinate s

$$\vec{m} = e^{i\beta} = \frac{\partial z_s}{\partial s} \tag{2}$$

$$\vec{n} = i\, e^{i\beta} = i\, \frac{\partial z_s}{\partial s} \tag{3}$$

in which $\cos\beta = \partial x_s/\partial s$ and $\sin\beta = \partial y_s/\partial s$ at a given time.

Assuming that the point on the curved shoreline moves normal to the shoreline due to erosion or accretion, the continuity equation for sediment can be written

$$\frac{\partial z_s}{\partial t} = \frac{1}{d}\left(\frac{\partial Q}{\partial s} + q_n\right)\vec{n} = \frac{i}{d}\left(\frac{\partial Q}{\partial s} + q_n\right)\frac{\partial z_s}{\partial s} \tag{4}$$

in which d = the depth of the active profile of the side slope of the causeway which is assumed to be displaced landward or seaward without change of the profile. Applying the empirical longshore sediment transport formula proposed by Komar and Inman (7) which is approximately the same as that in the Shore Protection Manual (17), the volumetric sediment transport rate along the causeway may be expressed as (13)

$$Q = Q_m \sin 2(\alpha_b + \beta) \tag{5}$$

with

$$Q_m = \frac{K H_b^{\,2}\sqrt{g H_b}}{16(s_s - 1)(1 - n_p)\sqrt{\kappa}} \tag{6}$$

in which $\beta = \mathrm{Arg}(\partial z_s/\partial s)$ from Eq. (2), H_b = the breaker height based on the root-mean-square wave characteristics, K = the dimensionless empirical constant, g = the gravitational acceleration, s_s = the specific gravity of the sediment relative to the fluid, n_p = the porosity of the sediment and κ = the ratio of H_b to the water depth at the breaker point ($\kappa \simeq 0.8$). In Eqs. (5) and (6) the

group velocity at the breaker point is approximated by $\sqrt{gH_b/\kappa}$ using shallow-water linear wave theory (13). The empirical constant in Eq. (6) is approximately given by $K \simeq 0.8$ for natural sand beaches. Determination of an appropriate value of K for a gravel causeway requires field data, but usual values are of the order of 0.8. $(\alpha_b+\beta)$ in Eq. (5) is the angle of wave incidence at the breaker point relative to the unit normal vector $\vec{n}$ at the location z_s assuming that the surf width is much smaller than the shoreline length. The value of $(\alpha_b+\beta)$ for natural sand beaches is normally small but that for a gravel causeway could be large. The present analysis is limited to the case of $-45° < (\alpha_b+\beta) < 45°$ so that the empirical formula given by Eqs. (5) and (6) may be applied. This limitation will be shown to be required for avoiding instability of shoreline evolution.

In order to compute the evolution of a curved shoreline with time, Eqs. (4) and (5) must be solved numerically for specified Q_m, α_b, q_n and d. The variation of z_s with respect to s yields the location of the curved shoreline at time t. The initial conditions required for the computation are expressed as

$$z_s = z_o = x_o + i\, y_o \quad , \quad s = s_o \qquad \text{at } t = 0 \tag{7}$$

in which the subscript 'o' denotes the quantities at t = 0 and z_o indicates the location of a point along the coordinate s_o following the initial shoreline. The numerical computation of $z_s(t,s)$ is difficult since the coordinate s following the instantaneous shoreline changes with time. It may be necessary to solve Eqs. (4) and (5) if the displacement of a curved shoreline is large as in the case of a large evolution of a curved spit.

In the following, Eqs. (4) and (5) will be shown to be approximated by Eqs. (15) and (16), respectively, if the displacement of the shoreline from the

initial position is small. For the case of small displacement, the location z_s at time t may approximately be expressed as

$$z_s \simeq z_o + \xi \vec{n}_o \tag{8}$$

in which ξ = the small displacement normal to the initial shoreline and ξ is positive for erosion and negative for accretion. $\vec{n}_o$ is the unit vector normal to the initial shoreline and given by

$$\vec{n}_o = i\, e^{i\beta_o} = i \frac{dz_o}{ds_o} \tag{9}$$

in which β_o = the value of β at t = 0 and z_o depends on s_o only. The assumption of the small displacement will be appropriate if the following conditions are satisfied

$$\frac{\partial \xi}{\partial s_o} << 1 \quad , \quad \frac{\xi}{R_o} << 1 \tag{10}$$

in which R_o is the radius of curvature of the initial shoreline and given by

$$R_o^{-1} = \frac{d\beta_o}{ds_o} = \mathrm{Im}\left(\frac{d\bar{z}_o}{ds_o} \frac{d^2 z_o}{ds_o^2}\right) \tag{11}$$

in which 'Im' indicates the imaginary part of the complex variable in the parentheses and $\bar{z}_o = (x_o - i\, y_o)$ is the complex conjugate of z_o. If the conditions given by Eq. (10) are satisfied, the relationship between the infinitesimal increments ds and ds_o can be approximated by

$$ds = \left[\left(\frac{\partial \xi}{\partial s_o}\right)^2 + \left(1 - \frac{\xi}{R_o}\right)^2\right]^{1/2} ds_o \simeq ds_o \tag{12}$$

in which the factor $(1 - \xi/R_o)$ accounts for the decrease of the radius of curvature of the shoreline from R_o to $(R_o - \xi)$ due to the small displacement ξ normal to the initial shoreline and the factor $(\partial \xi/\partial s_o)$ is related to the increment of ξ along the infinitesimal length ds_o. As a result, the dependent variables involved in the problem may be regarded to be a function of t and s_o

rather than t and s where s_o is independent of t.

Using Eqs. (9), (10) and (11), differentiation of Eq. (8) with respect to s_o yields

$$\frac{\partial z_s}{\partial s_o} \simeq \exp[i(\beta_o + \frac{\partial \xi}{\partial s_o})] \tag{13}$$

where $\partial\xi/\partial s_o$ is retained since β_o is arbitrary and may be much smaller than unity. Comparison of Eqs. (2) and (13) using Eq. (12) yields

$$\beta \simeq \beta_o + \frac{\partial \xi}{\partial s_o} \tag{14}$$

Differentiating Eq. (8) with respect to t and comparing the resulting equation with Eq. (4), the equation for the small displacement ξ is derived

$$\frac{\partial \xi}{\partial t} \simeq \frac{1}{d} (\frac{\partial Q}{\partial s_o} + q_n) \tag{15}$$

in which use is made of Eqs. (12) and (14). Substitution of Eq. (14) into Eq. (5) yields

$$Q \simeq Q_m[\sin 2(\alpha_b+\beta_o) + 2 \cos 2(\alpha_b+\beta_o) \frac{\partial \xi}{\partial s_o}] \tag{16}$$

Eqs. (15) and (16) may be solved numerically or analytically to derive the variation of the displacement ξ with time t along the coordinate s_o. The initial shoreline can be specified by describing the variation of z_o along the coordinate s_o. The variation of β_o along the coordinate s_o can be calculated using Eq. (9). The other necessary input parameters are Q_m, α_b, q_n and d which may vary with t along s_o. The initial condition for ξ is given by $\xi = 0$ at $t = 0$ since the coordinate s_o is taken to coincide with the initial shoreline. The boundary conditions for ξ must be given for a specific problem. For an initially straight shoreline s_o can be taken as $s_o = x$ and $\beta_o = 0$, so that Eqs. (15) and (16) become essentially the same as those used by previous investigators (8,9,10,13,14). Eqs. (15) and (16) are convenient for the analysis of

changes of curved shorelines since the present analysis utilizes the coordinate which follows the initial shoreline.

EROSION OF IDEALIZED CAUSEWAYS

Simple analytical and numerical solutions for an idealized causeway are obtained in the following. These solutions may be used for examining the accuracy of a numerical method for solving Eqs. (15) and (16) under more realistic conditions as well as for a preliminary assessment of the severity of erosion at the bend and the tip of the causeway. The idealized causeway analyzed in this paper is shown in Fig. 2 where s_o is the coordinate following the initial shoreline of the causeway exposed to wave attack. A sharp bend is located at $s_o = 0$ and the deflection angle of the bend is denoted by δ which is taken to be in the range $-90° < \delta < 90°$. The tip of the causeway is located at $s_o = -L$ and the width B of the causeway in the vicinity of the tip is assumed to be constant. The angle β_o between the x-axis and the unit vector tangent to the initial shoreline is given by $\beta_o = 0$ for $-L \leq s_o < 0$ and $\beta_o = \delta$ for $0 < s_o$ where the causeway is assumed to be infinitely long in the positive s_o-direction. The longshore sediment transport rate Q given by Eq. (16) is hence expressed as

$$Q_1 = Q_m(\sin 2\alpha_b + 2\cos 2\alpha_b \frac{\partial \xi_1}{\partial s_o}) \qquad (-L \leq s_o < 0) \tag{17}$$

$$Q_2 = Q_m[\sin 2(\alpha_b + \delta) + 2\cos 2(\alpha_b + \delta) \frac{\partial \xi_2}{\partial s_o}] \qquad (0 < s_o) \tag{18}$$

in which the subscripts '1' and '2' indicate the quantities corresponding to the regions $-L \leq s_o < 0$ and $0 < s_o$, respectively.

In order to obtain analytical solutions, Q_m and α_b are assumed to be constant neglecting wave transformations such as wave refraction and diffraction which is small due to the narrow surf zone on the causeway. Furthermore, the

depth d of the active profile of the side slope of the causeway may be assumed to be constant and taken such that $q_n \simeq 0$. Substitution of Eqs. (17) and (18) into Eq. (15) with $q_n \simeq 0$ yields

$$\frac{\partial \xi_1}{\partial t} = \varepsilon_1 \frac{\partial^2 \xi_1}{\partial s_o^2} \qquad (-L \leq s_o < 0) \tag{19}$$

$$\frac{\partial \xi_2}{\partial t} = \varepsilon_2 \frac{\partial^2 \xi_2}{\partial s_o^2} \qquad (0 < s_o) \tag{20}$$

with

$$\varepsilon_1 = 2 \frac{Q_m}{d} \cos 2\alpha_b \tag{21}$$

$$\varepsilon_2 = 2 \frac{Q_m}{d} \cos 2(\alpha_b + \delta) \tag{22}$$

The present analysis based on the empirical longshore sediment transport formula given by Eq. (5) is limited to the case of $0° < \alpha_b < 45°$ and $0 < (\alpha_b+\delta) < 45°$ so that $\varepsilon_1 > 0$ and $\varepsilon_2 > 0$ where α_b and δ are in degrees. The negative values of ε_1 and ε_2 would result in the instability of the shoreline evolution. The initial conditions for ξ_1 and ξ_2 are

$$\xi_1 = 0 \quad , \quad \xi_2 = 0 \qquad \text{at } t = 0 \tag{23}$$

The matching conditions at the sharp bend may be taken as

$$\xi_1 = \xi_2 \quad , \quad Q_1 = Q_2 \qquad \text{at } s_o = 0 \tag{24}$$

Since Q_2 approaches $Q_m \sin 2(\alpha_b+\delta)$ as s_o is increased, the boundary condition for ξ_2 is taken as

$$\frac{\partial \xi_2}{\partial s_o} \to 0 \qquad \text{as } s_o \to \infty \tag{25}$$

The boundary condition for ξ_1 at $s_o = -L$ depends on whether erosion or accretion occurs at the tip of the causeway. It will be shown in the example computation

that erosion or accretion will normally be confined in the vicinity of the bend and tip of the causeway. Consequently, the bend and the tip may be treated separately so long as the length L of the causeway between the bend and tip is sufficiently large. Correspondingly, the constant values of Q_m, α_b and d used in the following analyses for the bend and tip should be taken as the representative local values during a specified storm at the bend and tip, respectively.

Erosion at the Bend. - For the case of large L the value of Q_1 given by Eq. (17) approaches $Q_m \sin 2\alpha_b$ as s_o is decreased and the boundary condition may hence be approximated by

$$\frac{\partial \xi_1}{\partial s_o} \to 0 \qquad \text{as } s_o \to -\infty \tag{26}$$

The solutions of Eqs. (19) and (20) which satisfy the conditions given by Eqs. (23), (24), (25) and (26) can be written

$$\xi_1 = \xi_b \sqrt{\pi}\ \text{ierfc}\left(\frac{-s_o}{2\sqrt{\varepsilon_1 t}}\right) \qquad (0 \geq s_o) \tag{27}$$

$$\xi_2 = \xi_b \sqrt{\pi}\ \text{ierfc}\left(\frac{s_o}{2\sqrt{\varepsilon_2 t}}\right) \qquad (0 \leq s_o) \tag{28}$$

with

$$\xi_b = \sqrt{\frac{2Q_m t}{\pi d}}\ F \tag{29}$$

$$F = \frac{\sin 2(\alpha_b+\delta) - \sin 2\alpha_b}{\sqrt{\cos 2(\alpha_b+\delta)} + \sqrt{\cos 2\alpha_b}} \tag{30}$$

in which 'ierfc' is the notation for the integral of the complementary error function 'erfc' and is given by (1)

$$\text{ierfc}(\xi) = \int_\zeta^\infty \text{erfc}(x)\,dx = \frac{1}{\sqrt{\pi}} \exp(-\zeta^2) - \zeta\ \text{erfc}(\zeta) \tag{31}$$

Since ierfc(0) = $1/\sqrt{\pi}$, ξ_b defined by Eq. (29) is the displacement at $s_o = 0$ which is proportional to $\sqrt{t}$. Eqs. (27) and (28) can be shown to satisfy the overall conservation of sediment volume at the bend which can be expressed as

$$\int_{-\infty}^{0} d\xi_1 ds_o + \int_{0}^{\infty} d\xi_2 ds_o = Q_m[\sin 2(\alpha_b+\delta) - \sin 2\alpha_b]t \qquad (32)$$

Eqs. (27) and (28) indicate that the values of ξ_1/ξ_b and ξ_2/ξ_b decrease from unity at $s_o = 0$ to zero as s_o is decreased for ξ_1/ξ_b and increased for ξ_2/ξ_b. The effects of the bend are approximately limited to the region $-3.2\sqrt{\varepsilon_1 t} < s_o < 3.2\sqrt{\varepsilon_2 t}$ for which the values of ξ_1/ξ_b and ξ_2/ξ_b are greater than 0.01. If $\delta > 0$, ξ_1 and ξ_2 are positive and erosion will occur at the bend. If $\delta < 0$, ξ_1 and ξ_2 are negative and accretion will take place at the bend. Fig. 3 shows the variation of F with respect to α_b for $\delta = 10°$, $20°$, $30°$ and $40°$ where $F = 0$ for $\delta = 0°$. The values of F for $\delta < 0$ can be found using the relationship $F(\alpha_b,\delta) = -F(-\alpha_b,-\delta)$. It is assumed that $-45° < \alpha_b < (45°-\delta)$ for $0 \leq \delta < 90°$ and $-(45°+\delta) < \alpha_b < 45°$ for $-90° < \delta < 0°$ so that ε_1 and ε_2 given by Eqs. (21) and (22) are positive. For $0° < \delta \leq 30°$ F is maximum at $\alpha_b = -\delta/2$ and the maximum value of $F = \sin\delta/\sqrt{\cos\delta}$. For $30° < \delta < 90°$ F is maximum at $\alpha_b = -45°$ and $(45°-\delta)$ and the maximum value of $F = \sqrt{2\tan\delta}\,\sin\delta$. Since ξ_b is given by Eq. (29), the maximum displacement ξ_b at the bend is not very sensitive to α_b for the range of α_b considered in this analysis. Since ξ_b increases as δ is increased from zero, the severity of erosion at the bend deflected onshore towards the direction of wave propagation for which $\delta > 0$ increases as the positive deflection angle of the bend is increased.

Erosion at the Tip. - Erosion at the tip of the causeway will be shown to occur if $\alpha_b > 0$. Introducing the coordinate $z = (s_o+L)$, the tip and the bend are located at $z = 0$ and $z = L$, respectively. For the case of large L and $\alpha_b > 0$

the boundary conditions for ξ_1 may be taken as

$$Q_1 = 0 \qquad \text{at } z = 0 \tag{33}$$

$$\frac{\partial \xi_1}{\partial z} \to 0 \qquad \text{as } z \to \infty \tag{34}$$

in which Q_1 is given by Eq. (17). The solution of Eq. (19) with $z = (s_o+L)$ which satisfies the conditions given by Eqs. (23), (33) and (34) can be written

$$\xi_1 = \xi_t \sqrt{\pi}\ \text{ierfc}\left(\frac{z}{2\sqrt{\varepsilon_1 t}}\right) \qquad (0 \le z) \tag{35}$$

with

$$\xi_t = \sqrt{\frac{2Q_m t}{\pi d}}\ \frac{\sin 2\alpha_b}{\sqrt{\cos 2\alpha_b}} \tag{36}$$

in which ξ_t is the value of ξ_1 at $z = 0$ and positive for $0 < \alpha_b < 45°$ where the present analysis is limited to the case of $\varepsilon_1 > 0$. The value of ξ_1/ξ_t decreases from unity at $z = 0$ to zero as z is increased. If $\alpha_b > 0$, erosion will occur approximately in the region $0 \le z < 3.2\sqrt{\varepsilon_1 t}$ for which ξ_1/ξ_t is greater than 0.01. The maximum erosion ξ_t at the tip increases rapidly as α_b is increased from zero to 45°. It should be noted that the solution given by Eq. (35) may also be applied if the side slope of the causeway for the region $z < 0$ is protected so that $Q_1 = 0$ for $z < 0$ but that for the region $z > 0$ is not protected and $Q_1 > 0$ for $z > 0$. This implies that erosion at the tip of the causeway is mathematically similar to that at the transition point between the protected and unprotected regions.

ξ_t given by Eq. (36) increases with time and becomes equal to the width B of the causeway in the vicinity of the tip at $t = t_r$ where t_r is given by

$$t_r = \frac{\pi d B^2}{2Q_m}\ \frac{\cos 2\alpha_b}{\sin^2 2\alpha_b} \tag{37}$$

For $t > t_r$, ξ_1 is no longer given by Eq. (35) since the displacement ξ_1 is limited by B. Defining the receding point as the point where $\xi_1 = B$, the receding point moves with time in the positive z-direction. Denoting the unknown location of the receding point by $z = r(t)$ for $t \geq t_r$, the boundary condition for ξ_1 given by Eq. (33) must be modified as

$$Q_1 = 0 \quad , \quad \xi_1 = B \qquad \text{at } z = r(t) \tag{38}$$

Eq. (19) with $z = (s_o+L)$ together with Eqs. (34) and (38) are solved numerically to obtain the values of ξ_1 and r for $t \geq t_r$.

For convenience of the numerical computation the following dimensionless variables are introduced

$$t_* = \frac{t}{t_r} - 1 \quad , \; z_* = \frac{z}{z_c} \quad , \; \xi_* = \frac{\xi_1}{B} \quad , \quad r_* = \frac{r}{z_c} \tag{39}$$

with

$$z_c = \frac{\pi}{2} B \cot 2\alpha_b \tag{40}$$

in which the subscript '*' indicates the dimensionless variables and $z_c > 0$ since the present analysis is limited to the range $0 < \alpha_b < 45°$. Substitution of Eq. (39) into Eqs. (19), (34) and (38) yields

$$\frac{\partial \xi_*}{\partial t_*} = \frac{4}{\pi} \frac{\partial^2 \xi_*}{\partial z_*^2} \qquad (z_* > r_*, \; t_* > 0) \tag{41}$$

$$\frac{\partial \xi_*}{\partial z_*} \to 0 \qquad \text{as } z_* \to \infty \tag{42}$$

$$\frac{\partial \xi_*}{\partial z_*} = -\frac{\pi}{4} \quad , \quad \xi_* = 1 \qquad \text{at } z_* = r_*(t_*) \tag{43}$$

Since ξ_1 is given by Eq. (35) at $t = t_r$, the initial conditions for ξ_* and r_* at $t_* = 0$ can be written

$$\xi_* = \sqrt{\pi}\ \text{ierfc}\ (\frac{\sqrt{\pi}}{4} z_*) \quad , \quad r_* = 0 \qquad \text{at } t_* = 0 \tag{44}$$

The steady solution of this receding boundary problem in terms of the moving coordinate (z_*-r_*) for large t_* may be shown to exist and be given by

$$\xi_* = \exp[-\frac{\pi}{4}(z_* - r_*)] \ , \ \frac{dr_*}{dt_*} = 1 \qquad \text{for large } t_* \tag{45}$$

After the steady state relative to the receding point is reached, the receding rate given by Eq. (45) can be rearranged to $dr/dt = [Q_m \sin 2\alpha_b/(dB)]$ where use is made of Eqs. (37), (39), (40) and (45). This implies that the rate of sediment volume eroded at the receding front equals the longshore sediment transport rate along the straight segment of the causeway.

Eq. (41) with Eqs. (42)-(44) is solved numerically using the finite element computer program developed for the analysis of thermoerosion of frozen soil by Kobayashi and Aktan (5). The present problem is mathematically similar to the problem of heat conduction with phase changes except that the term corresponding to the latent heat of fusion is not included in the present problem. Fig. 4 shows the computed variation of r_* with respect to t_*. Fig. 5 shows the computed variation of ξ_* as a function of z_* for $t_* = 0$, 0.6, 1.2 and 2.0. In order to check the accuracy of the computation, the computation is made starting from $t_* = -1$, that is, $t = 0$. The differences between the computed values of ξ_* for $-1 \leq t_* \leq 0$ and the exact values obtained from Eq. (35) are less than 0.03. Fig. 4 indicates that dr_*/dt_* is approximately unity for $t_* > 2.0$. The computed variations of ξ_* with respect to z_* for $t_* > 2.0$ are found to be well represented by the steady solution given by Eq. (45). Consequently, the steady state relative to the receding front is approximately reached for $t_* > 2.0$. For $t_* > 2$, ξ_* is approximately given by Eq. (45) with $r_* \simeq [1.73 + (t_* - 2)]$.

Finally, if $\alpha_b < 0$, accretion will occur at the tip of the causeway. If the boundary condition at the tip is to be taken as $\partial Q_1/\partial z = 0$ at $z = 0$, the solution of Eq. (19) with $z = s_o + L$ which satisfies this boundary condition, the boundary condition given by Eq. (34) and the initial condition $\xi_1 = 0$ at $t = 0$ will simply be given by $\xi_1 = 0$ and hence $Q_1 = Q_m \sin 2\alpha_b$ for $z \geq 0$. This solution implies that for the region $z \geq 0$ the causeway will remain essentially straight and the rate of sediment volume deposited in the region $z < 0$ will be equal to the rate of longshore sediment transport along the straight segment of the causeway. However, a more detailed analysis including the effects of wave refraction and diffraction is required to predict the accretion pattern at the tip of the causeway.

EXAMPLE COMPUTATION

Computation is made to estimate the severity of erosion of an unprotected causeway in the southern Beaufort Sea. For lack of available data the empirical constant K in Eq. (6) is assumed to be $K = 0.8$ which is obtained for natural sand beaches (7). The typical value of the parameter κ in Eq. (6) is usually taken as $\kappa = 0.8$ although the value of κ depends on the slope and the steepness of incident waves (13,17). The specific gravity and the porosity of the fill material of the causeway are assumed to be $s_s = 2.6$ and $n_p = 0.4$ which may be appropriate for gravel in sea water. The limitations of the empirical longshore sediment transport formula given by Eqs. (5) and (6) are that it does not account for the side slope of the causeway and the size of the fill material. Applying the equilibrium beach profile model proposed by Dean (3), the equilibrium profile of a gravel beach under the action of waves of normal incidence may have an average slope of approximately 1:5. The change of the side slope profile of the causeway during a storm is not considered in the present analysis but could be

investigated using the analysis procedure based on the equilibrium beach profile concept (3) if waves are of normal incidence. The breaker height H_b based on the root-mean-square wave characteristics is taken as H_b = 5 ft (1.5 m) which appears to be a typical value in the shallow water of the southern Beaufort Sea during an occasional severe storm (6). The associated wave period may be of the order 5 sec but the present simple analysis does not account for the wave period effects. Eq. (6) with K = 0.8, κ = 0.8, s_s = 2.6, n_p = 0.4 and H_b = 5 ft (1.5 m) yields Q_m = 18.5 ft^3/sec (0.523 m^3/sec).

The height and configuration of the causeway depend on site-specific conditions. The tip of the causeway may be located in water depth as large as 12 ft (3.7 m) (2). The storm surge associated with a storm of 100-year return period was estimated to be 6-7 ft (1.8-2.1 m) (15). In the following computation the height d of the active profile of the side slope of the causeway is assumed to be the same as the height of the causeway above the seabed which is taken to be 25 ft (7.6 m) considering the typical design values of the water depth, storm surge including minor effects of tides, and wave runup and overtopping. Field data on the eroded profile of the side slope is required for accurately determining the value of d such that $q_n \simeq 0$ at the water depth of closure of the analysis domain which is typically estimated at 30 ft (9.1 m) for the analysis of shoreline evolution (9). Gravel grains on the side slope of the causeway in shallow water will be moved by waves during an occasional severe storm in the southern Beaufort Sea (6).

Fig. 6 shows the variations of the shoreline displacements ξ_1 and ξ_2 computed using Eqs. (27) and (28) at the bend of the deflection angle $\delta = 10°$ for t = 1, 4, 9 and 16 hr where use is made of Q_m = 18.5 ft^3/sec (0.523 m^3/sec), d = 25 ft (7.6 m) and $\alpha_b = 15°$. Fig. 3 indicates that the computed results will not be very sensitive to the value of α_b so long

as $\delta = 10°$ and α_b is in the range $-45° < \alpha_b < 35°$. Fig. 6 suggests that erosion at the bend may be severe but confined in the vicinity of the bend. Fig. 7 shows the variation of the displacement ξ_1 computed using Eq. (35) at the tip of the causeway for t = 1, 4, 9 and 16 hr where the values of Q_m, d and α_b at the tip are assumed to be the same as those at the bend although this assumption is not necessary since the bend and the tip have been analyzed separately. The minimum length L between the bend and the tip required for the separate treatment of the bend and the tip can be estimated for given time using Figs. 6 and 7. If the width of the causeway at the tip is less than the value of ξ_1 at z = 0 for given time in Fig. 7, additional computation using Figs. 4 and 5 will be required. Fig. 7 suggests that erosion at the tip may also be severe but confined in the vicinity of the tip. Since erosion at the tip is sensitive to the value of α_b, a detailed wave refraction computation is required for predicting the severity of erosion at the tip using site-specific data. Fig. 7 also indicates the degree of erosion expected in the unprotected region $z > 0$ next to the protected region $z < 0$ although slumping of the fill material in the protected region may reduce the severity of erosion. It should be noted that the present analysis is limited to the case of unfrozen soil. Erosion as severe as that shown in Fig. 7 may result in exposure of frozen soil to wave action where the frozen soil may exist at the depth of approximately 8 ft (2.4 m) below the surface of the causeway. The analysis of thermoerosion of frozen soil due to wave action by Kobayashi and Aktan (5) indicates that the frozen soil may not reduce erosion significantly.

SUMMARY AND CONCLUSION

Erosion of an unprotected gravel causeway with a relatively gentle side slope caused by the variation of sediment transport rates along the causeway due

to breaking waves is analyzed using the coordinate following the initial shoreline of the causeway and the longshore sediment transport formula originally developed for natural sand beaches. An analytical solution for erosion at the bend of a long causeway is obtained neglecting wave transformations in the vicinity of the bend. Analytical and numerical solutions for erosion and recession of the tip of a long causeway are also presented neglecting the effects of wave diffraction and refraction and development of longshore current (6) at the tip of the causeway. An example computation based on these simple solutions is made for a hypothetical unprotected causeway in the southern Beaufort Sea. The computation indicates that erosion due to an occasional severe storm may be severe but limited in the vicinity of the bend and the tip, respectively. The analysis also suggests that if a slope protection system is provided to a limited region of a causeway, erosion of the unprotected region next to the protected region could be similar to that of the tip of an unprotected causeway.

Field data are needed to verify the applicability of the longshore sediment transport formula for natural sand beaches to gravel causeways as well as to calibrate the parameters involved in the formula. Admittedly, the present analysis assumes that a gravel causeway is similar to a spit with sand beaches. A more rigorous approach would require detailed analyses of wave and current fields and sediment transport due to the combined wave and current action. However, extensive computational efforts would be necessary for the detailed analyses. Alternatively, a computer program based on the present approach including the effects of wave transformations, frozen soil and the change of the side slope profile may be developed to predict erosion of the causeway in a more realistic manner although field data are still needed to establish sediment transport relationships. The analytical solutions presented in this paper can be used to examine the accuracy of such a computer program.

ACKNOWLEDGMENTS

This project is partly supported by the University of Delaware Sea Grant Program.

APPENDIX I. - REFERENCES

1. Abramowitz, M., and Stegun, I. A., Handbook of Mathematical Functions, Dover, New York, 1972.

2. Cox, J. C., and Machemehl, J. L., "Hydraulic Model Testing of an Arctic Seawater Intake Structure," Proceedings of Coastal Structures '83, ASCE, 1983, pp. 532-550.

3. Dean, R. G., "Shoreline Erosion due to Extreme Storms and Sea Level Rise," Report No. UFL/COEL-83/007, Coastal and Oceanographic Engineering Department, University of Florida, Gainesville, Florida, 1983.

4. Hume, J. D., and Schalk, M., "Shoreline Processes Near Barrow, Alaska: A Comparison of the Normal and the Catastrophic," Arctic, Vol. 20, 1967, pp. 86-103.

5. Kobayashi, N., and Aktan, D., "Thermoerosion of Frozen Sediment Under Wave Action," Journal of Waterway, Port, Coastal and Ocean Engineering, Vol. 112, No. 1, 1986, pp. 140-158.

6. Kobayashi, N., Vivatrat, V., Madsen, O. S., and Boaz, I. B., "Erosion Prediction for Exploration and Production Structures in the Arctic," OTC Paper 4114, 13th Offshore Technology Conference, Houston, Texas, 1981.

7. Komar, P. D., and Inman, D. L., "Longshore Sand Transport on Beaches," Journal of Geophysical Research, Vol. 75, No. 30, 1970, pp. 5914-5927.

8. Komar, P. D., Beach Processes and Sedimentation, Prentice-Hall, Englewood Cliffs, New Jersey, 1976.

9. Le Mehaute, B., and Soldate, M., "Mathematical Modeling of Shoreline Evolution," Proceedings of 16th Coastal Engineering Conference, Vol. II, ASCE, 1978, pp. 1163-1179.

10. Le Mehaute, B., Wang, J. D., and Lu, C. C., "Wave Data Discretization for Shore Line Processes," Journal of Waterway, Port, Coastal and Ocean Engineering, Vol. 109, No. 1, 1983, pp. 63-78.

11. Nummedal, D., "Coarse Grained Sediment Dynamics - Beaufort Sea, Alaska," Proceedings of Port and Ocean Engineering Under Arctic Conditions, Norwegian Institute of Technology, Trondheim, Norway, 1979, pp. 845-858.

12. Owens, E. H., Harper, J. R., and Nummedal, D., "Sediment Transport Processes and Coastal Variability on the Alaskan North Slope," Proceedings of 17th Coastal Engineering Conference, Vol. II, ASCE, 1980, pp. 1344-1363.

13. Perlin, M., and Dean, R. G., "Prediction of Beach Planforms with Littoral Controls," Proceedings of 16th Coastal Engineering Conference, Vol. II, ASCE, 1978, pp. 1818-1838.

14. Perlin, M., and Dean, R. G., "A Numerical Model to Simulate Sediment Transport in the Vicinity of Structures," Miscellaneous Report No. 83-10, U.S. Army Corps of Engineers, Coastal Engineering Research Center, Ft. Belvoir, Va., 1983.

15. Reimnitz, E., and Maurer, D. K., "Storm Surges in the Alaskan Beaufort Sea," Open-File 78-593, U.S. Geological Survey, Menlo Park, Calif., 1978.

16. Short, A. D., Coleman, J. M., and Wright, L. D., "Beach Dynamics and Nearshore Morphology of the Beaufort Sea Coast, Alaska," Proceedings of the Arctic Institute of North America, Symposium on Beaufort Sea Coast and Shelf Research, Arlington, Va., 1974, pp. 477-488.

17. U.S. Army Coastal Engineering Research Center, Shore Protection Manual, Vol. 1, U.S. Government Printing Office, Washington, D.C., 1977.

APPENDIX II. - NOTATION

The following symbols are used in this paper:

B = width of causeway;

d = height of active profile of side slope of causeway;

erfc = complementary error function;

F = function defined by Eq. (30);

g = gravitational acceleration;

H_b = breaker height based on root-mean-square wave characteristics;

i = imaginary unit;

ierfc = integral of complementary error function;

K = empirical constant in Eq. (6);

L = length between bend and tip of causeway;

$\vec{m}$ = unit tangential vector;

$\vec{n}$ = unit normal vector;

$\vec{n}_o$ = unit vector normal to initial shoreline;

n_p = porosity of sediment;

Q = volumetric longshore sediment transport rate;

Q_m = parameter defined by Eq. (6);

Q_1 = sediment transport rate given by Eq. (17);

Q_2 = sediment transport rate given by Eq. (18);

q_n = volumetric offshore sediment transport rate per unit shoreline length;

R_o = radius of curvature of initial shoreline;

r = location of receding point;

r_* = normalized location of receding point defined by Eq. (39);

s = coordinate following instantaneous shoreline;

s_o = coordinate following initial shoreline;

s_s = specific gravity of sediment;

t = time;

t_r = time when recession of tip starts;

t_* = normalized time defined by Eq. (39);

x = fixed Cartesian coordinate;

x_o = x-coordinate of a point on initial shoreline;

x_s = x-coordinate of a point on instantaneous shoreline;

y = fixed Cartesian coordinate;

y_o = y-coordinate of a point on initial shoreline;

y_s = y-coordinate of a point on instantaneous shoreline;

z = coordinate whose origin is located at tip of causeway;

z_c = characteristic length defined by Eq. (40);

z_o = location of a point on initial shoreline;

$\overline{z}_o$ = complex conjugate of z_o;

z_s = location of a point on instantaneous shoreline;

z_* = normalized coordinate defined by Eq. (39);

α_b = angle of wave incidence at breaker point relative to y-axis;

β = angle between $\vec{m}$ and x-axis;

β_o = value of β corresponding to initial shoreline;

δ = deflection angle of bend;

ε_1 = parameter defined by Eq. (21);

ε_2 = parameter defined by Eq. (22);

κ = ratio of breaker height to water depth at breaker point;

ξ = small displacement normal to initial shoreline;

ξ_b = shoreline displacement at bend of causeway;

ξ_t = shoreline displacement at tip of causeway;

ξ_1 = shoreline displacement between bend and tip;

ξ_2 = shoreline displacement from bend to large s_o; and

ξ_* = normalized displacement defined by Eq. (39).

LIST OF FIGURES

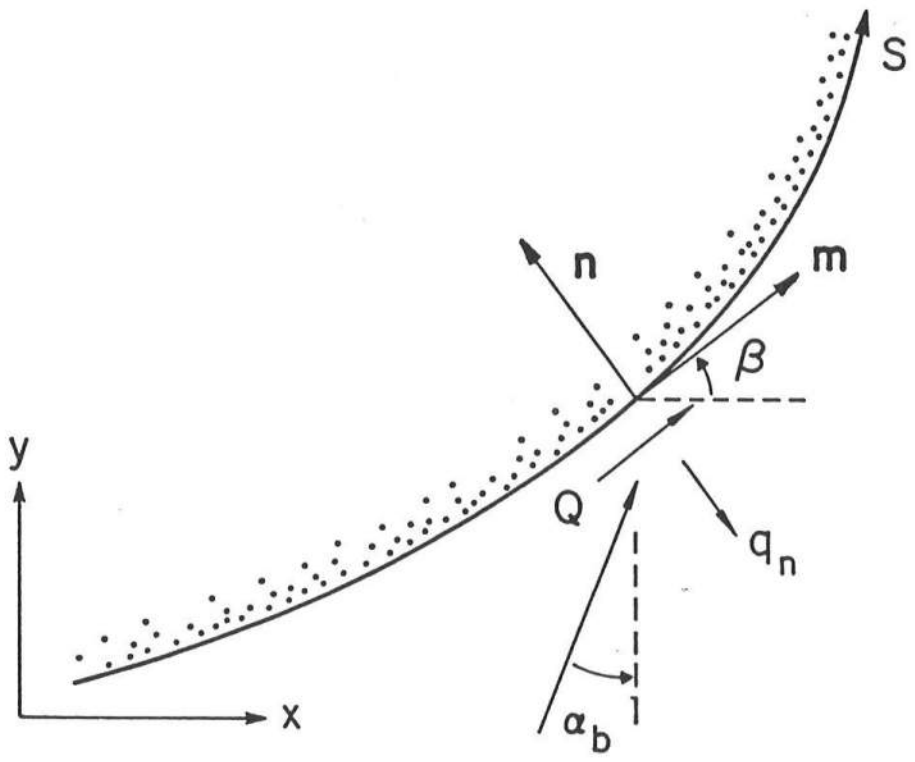

Fig. 1 Definition Sketch

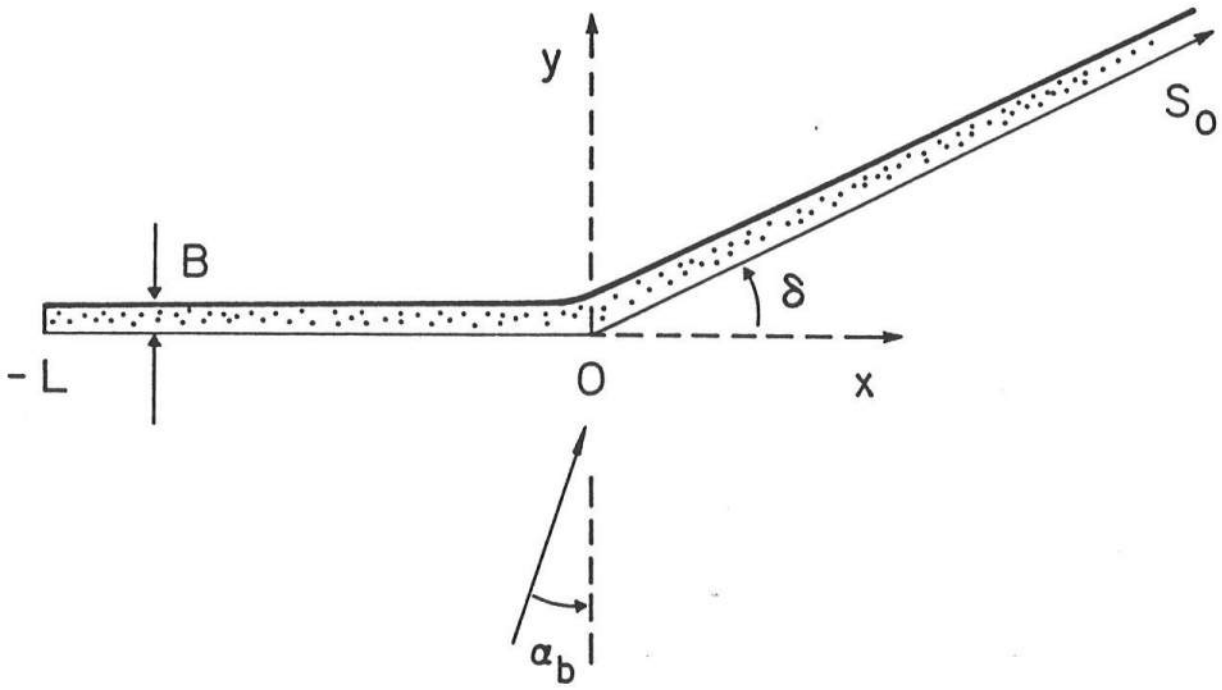

Fig. 2 An Idealized Causeway

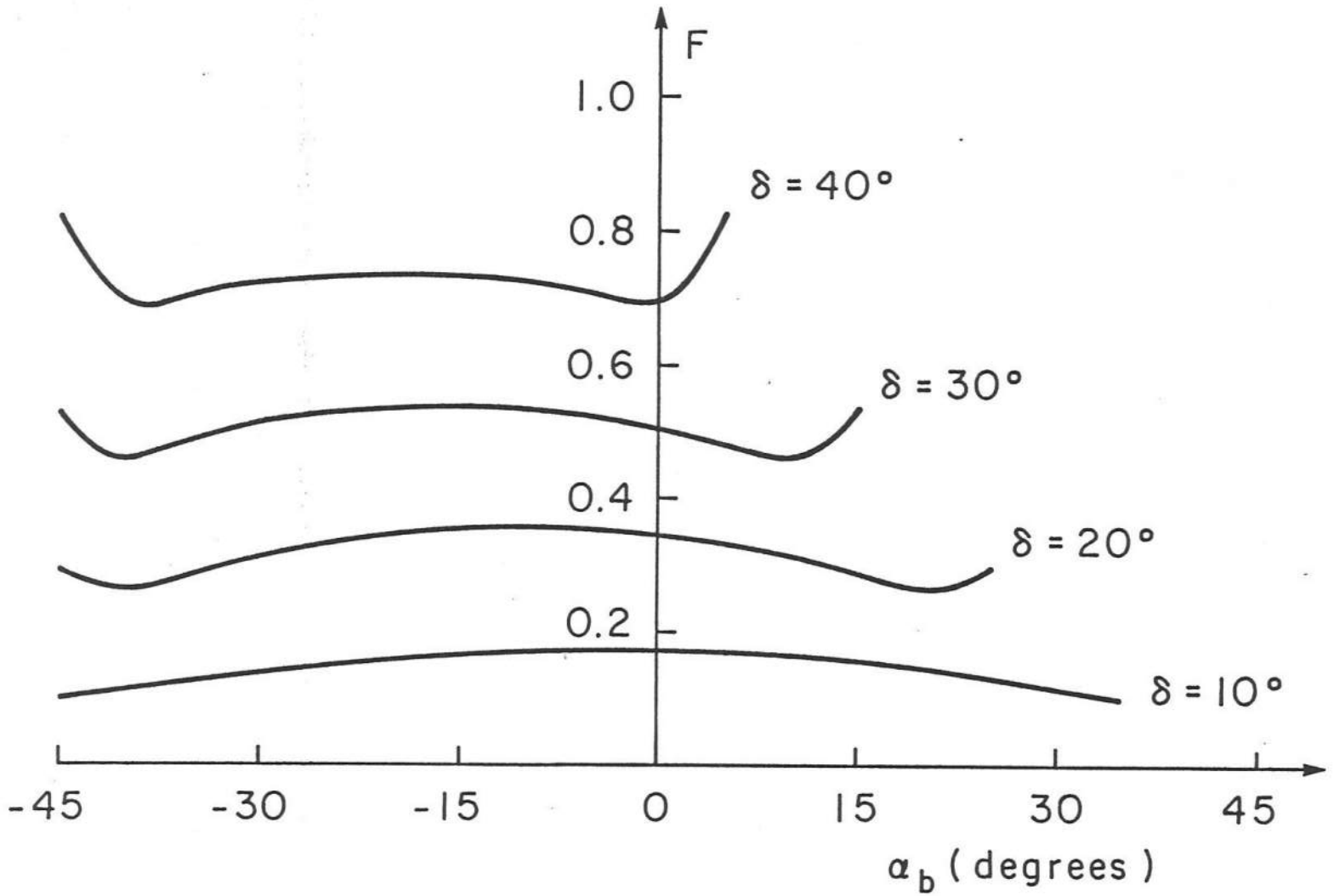

Fig. 3 F as a Function of α_b and δ

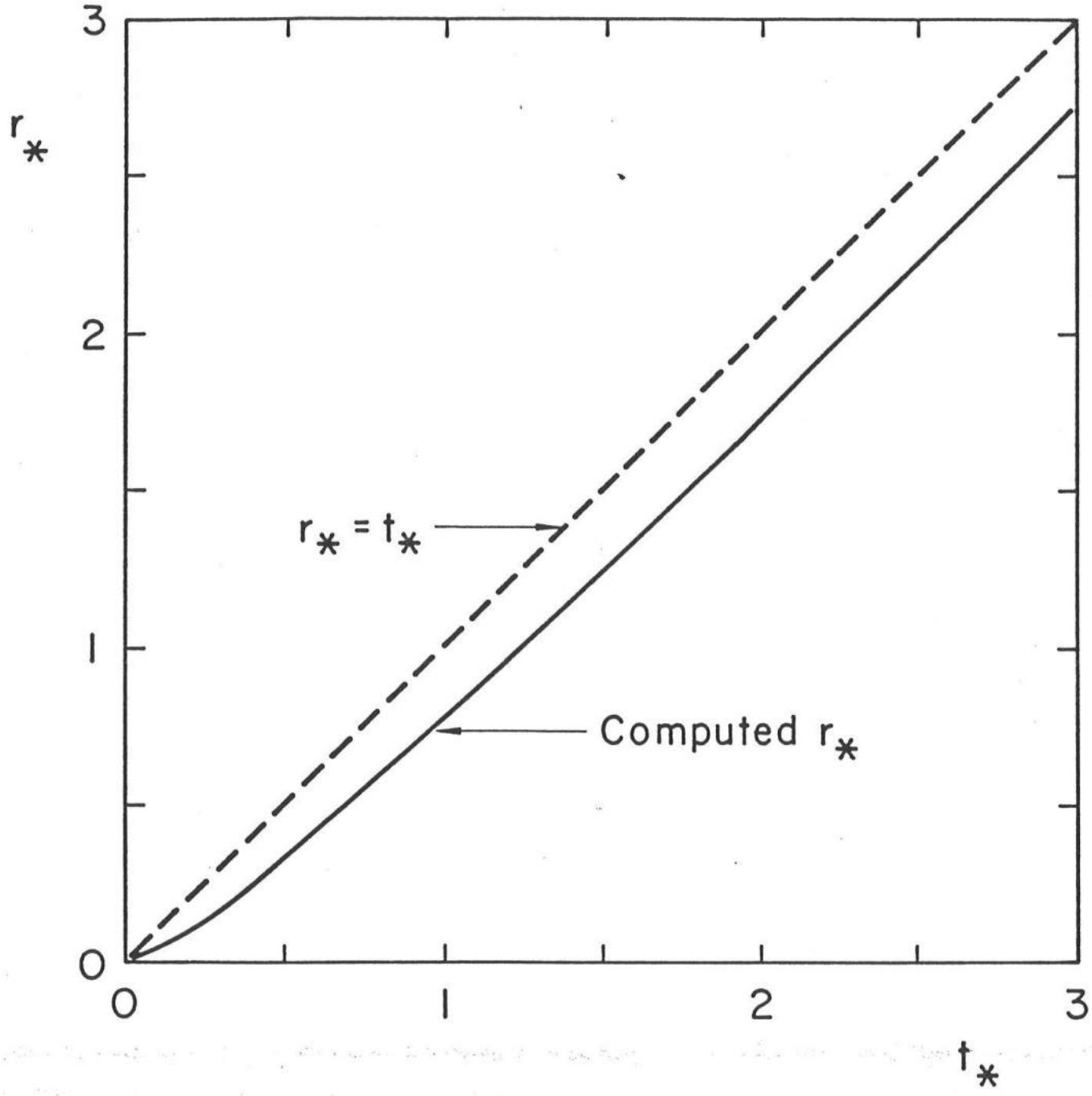

Fig. 4 Normalized Location of Receding Point

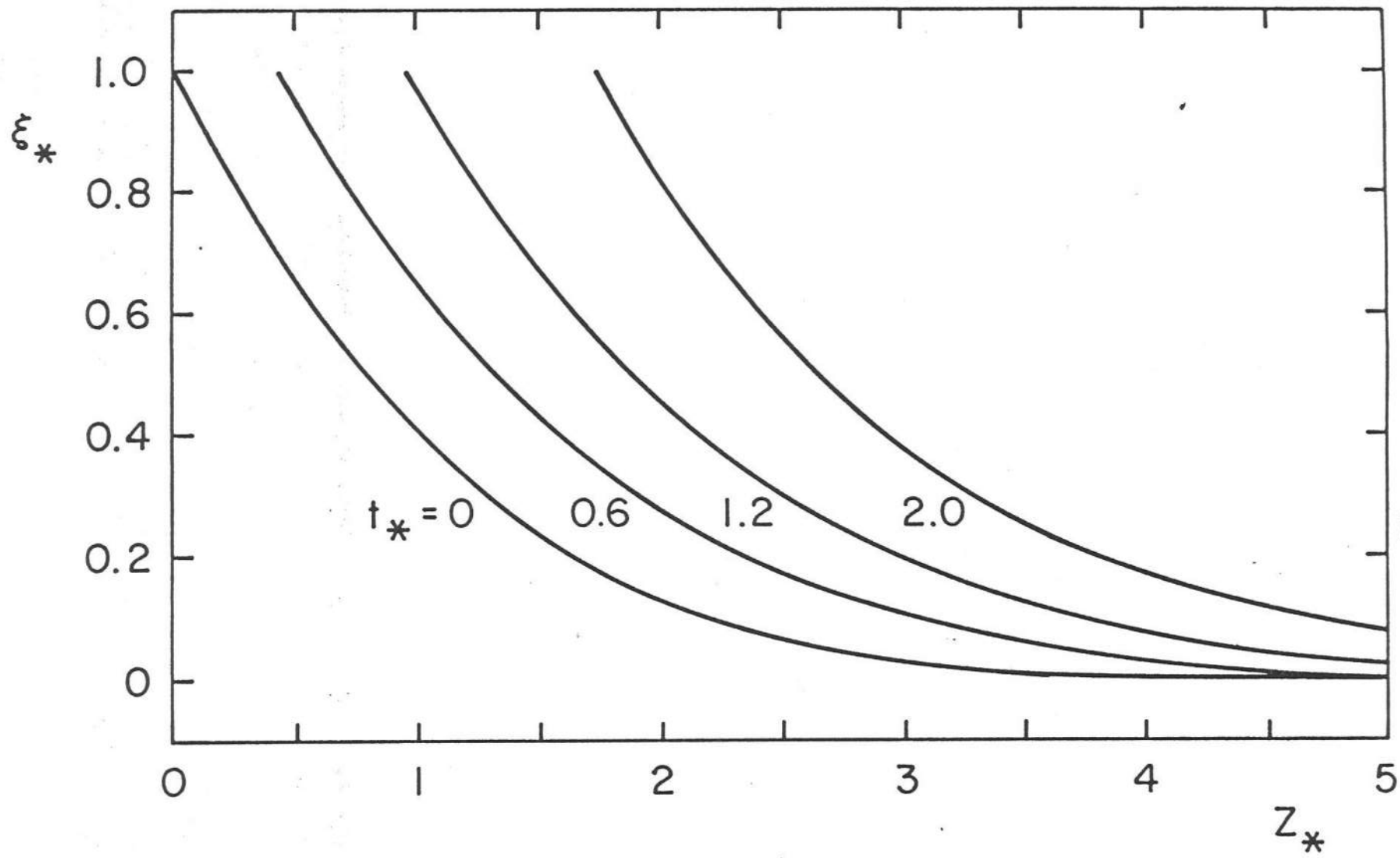

Fig. 5 Normalized Shoreline Displacement in the Vicinity of Receding Point

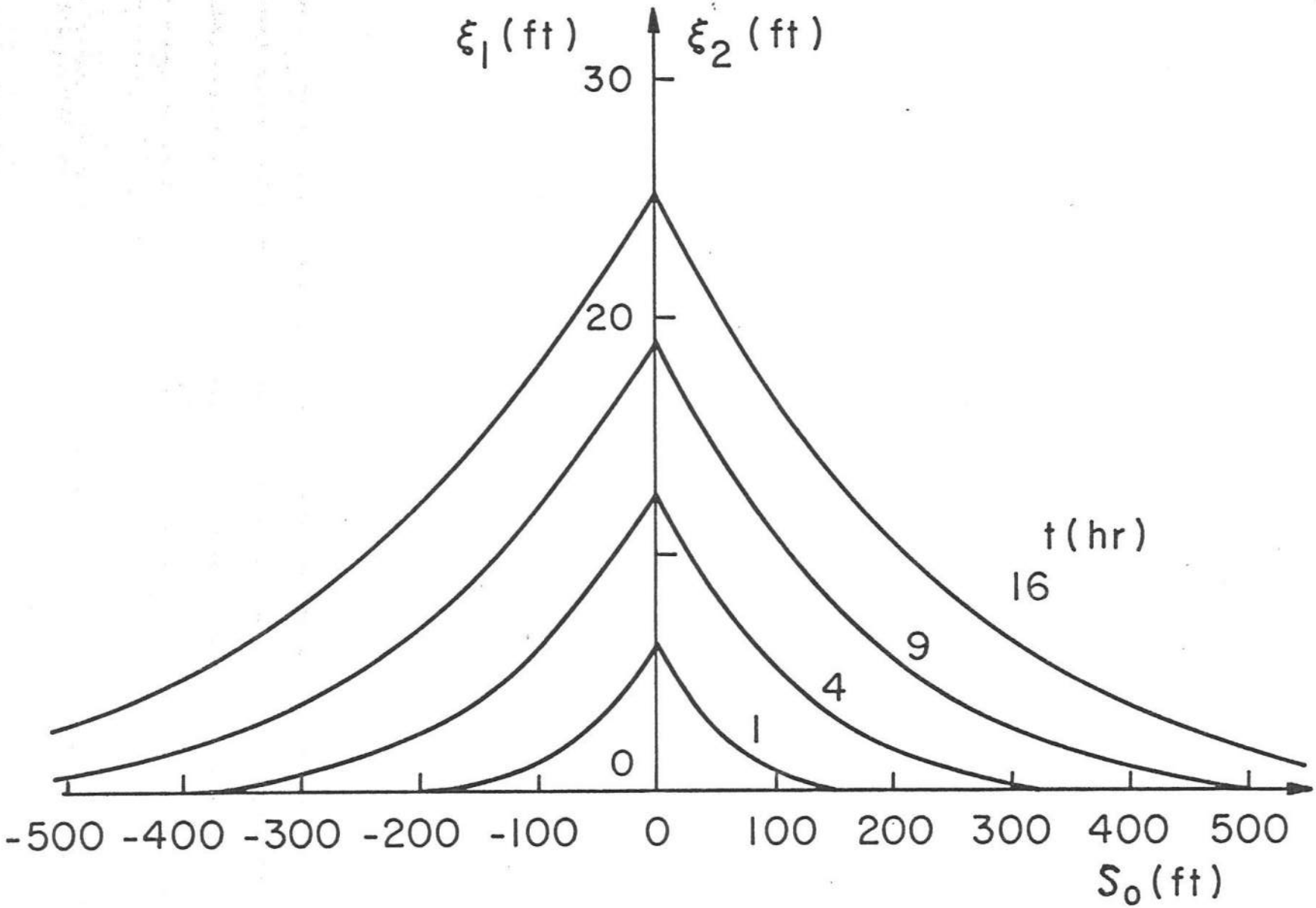

Fig. 6 Erosion at the Bend of an Example Causeway (Note: 1 ft = 0.305 m)

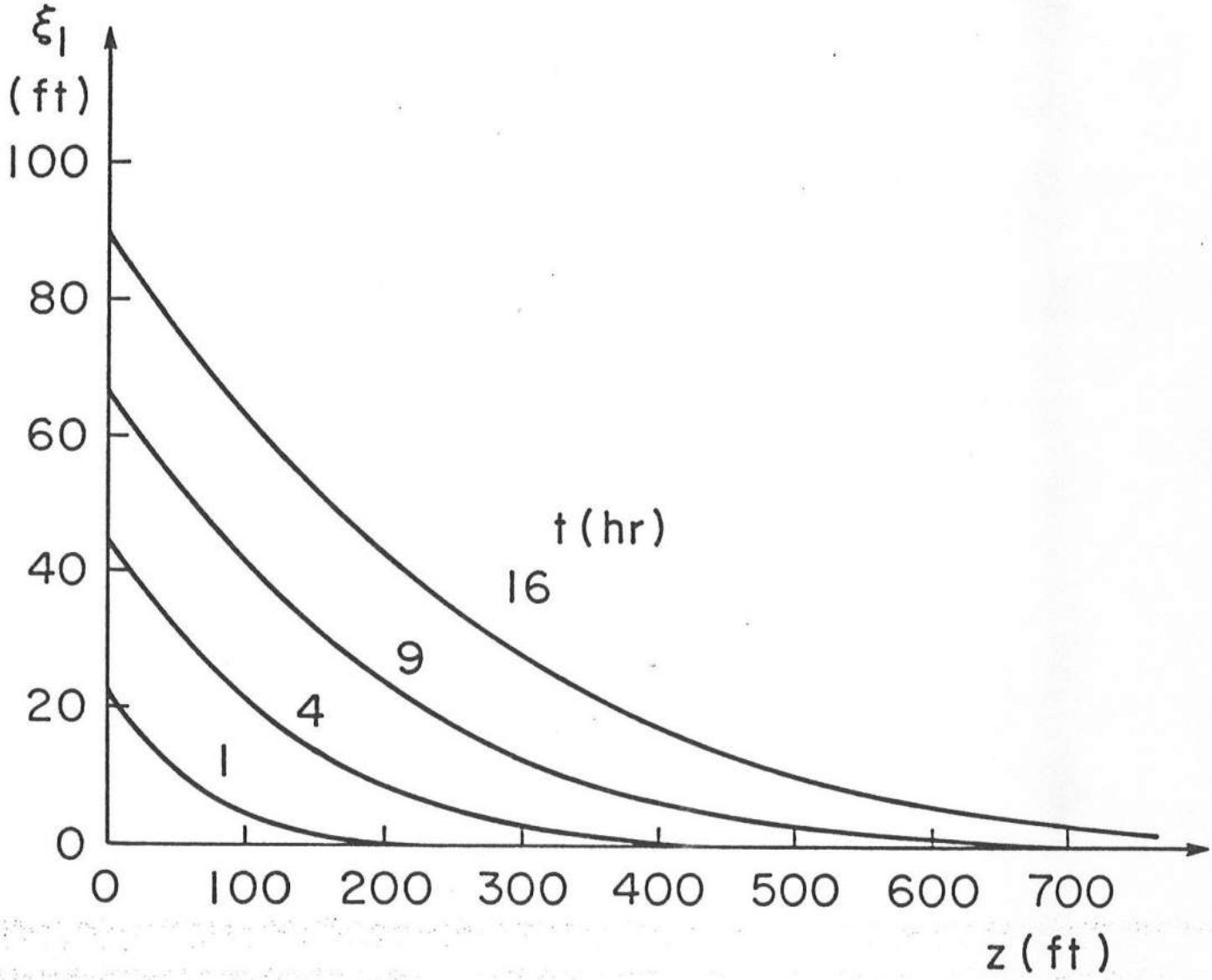

Fig. 7 Erosion at the Tip of an Example Causeway (Note: 1 ft = 0.305 m)